Title
Direct Visualization of Individual Aromatic Compound Structures in Low Molecular Weight Marine Dissolved Organic Carbon

Journal
Geophysical Research Letters, 45(11)

ISSN
0094-8276

Authors
Fatayer, Shadi
Coppola, Alysha I
Schulz, Fabian
et al.

Publication Date
2018-06-16

DOI
10.1029/2018gl077457

Peer reviewed

AGU100 ADVANCING EARTH AND SPACE SCIENCE

Geophysical Research Letters

RESEARCH LETTER
10.1029/2018GL077457

Shadi Fatayer and Alysha I. Coppola contributed equally to this work.

Key Points:
- Real-space visualization of single molecules in low molecular weight marine dissolved organic carbon (LMW DOC) is demonstrated using atomic force microscopy
- Comparison between surface and deep LMW DOC reveals a greater fraction of aromatic structures in the deep ocean
- Identified compounds are generally similar to black carbon, polycyclic aromatic compounds, and carboxylic-rich alicyclic molecules (CRAM)

Supporting Information:
- Supporting Information S1
- Data Set S1
- Data Set S2
- Data Set S3
- Data Set S4
- Data Set S5
- Data Set S6
- Data Set S7
- Data Set S8
- Data Set S9
- Data Set S10
- Data Set S11
- Data Set S12
- Data Set S13
- Data Set S14
- Data Set S15
- Data Set S16
- Data Set S17
- Data Set S18
- Data Set S19
- Data Set S20
- Data Set S21
- Data Set S22
- Data Set S23
- Data Set S24
- Data Set S25

Correspondence to:
A. I. Coppola and L. Gross,
lgr@zurich.ibm.com;
alysha.coppola@geo.uzh.ch

Citation:
Fatayer, S., Coppola, A. I., Schulz, F., Walker, B. D., Broek, T. A., Meyer, G., et al. (2018). Direct visualization of individual aromatic compound structures in low molecular weight marine dissolved organic carbon. *Geophysical Research Letters*, *45*, 5590–5598. https://doi.org/10.1029/2018GL077457

Received 5 FEB 2018
Accepted 25 APR 2018
Published online 5 JUN 2018

Direct Visualization of Individual Aromatic Compound Structures in Low Molecular Weight Marine Dissolved Organic Carbon

Shadi Fatayer[1], Alysha I. Coppola[2], Fabian Schulz[1], Brett D. Walker[3], Taylor A. Broek[4], Gerhard Meyer[1], Ellen R. M. Druffel[3], Matthew McCarthy[4], and Leo Gross[1]

[1]IBM Research – Zurich, Rüschlikon, Switzerland, [2]Department of Geography, University of Zurich, Zurich, Switzerland, [3]Department of Earth System Science, University of California, Irvine, CA, USA, [4]Department of Ocean Science, University of California, Santa Cruz, CA, USA

Abstract Dissolved organic carbon (DOC) is the largest pool of exchangeable organic carbon in the ocean. However, less than 10% of DOC has been molecularly characterized in the deep ocean to understand DOC's recalcitrance. Here we analyze the radiocarbon (^{14}C) depleted, and presumably refractory, low molecular weight (LMW) DOC from the North Central Pacific using atomic force microscopy to produce the first atomic-resolution images of individual LMW DOC molecules. We evaluate surface and deep LMW DOC chemical structures in the context of their relative persistence and recalcitrance. Atomic force microscopy resolved planar structures with features similar to polycyclic aromatic compounds and carboxylic-rich alicyclic structures with less than five aromatic carbon rings. These compounds comprise 8% and 20% of the measurable molecules investigated in the surface and deep, respectively. Resolving the structures of individual DOC molecules represents a step forward in molecular characterization of DOC and in understanding its long-term stability.

Plain Language Summary The marine dissolved organic carbon (DOC) reservoir is similar in size to that of atmospheric carbon dioxide and plays an important role in the ocean carbon cycle. DOC comprises a vast mixture of diverse molecules, the majority of which remain structurally uncharacterized. Identification of DOC molecular structures will aid our understanding of DOC cycling. Here, we present the first images of individual DOC molecules using atomic force microscopy. We compare images of low molecular weight DOC molecules extracted from samples collected at different depths in the North Central Pacific. Our results help unravel the molecular architecture, formation processes, and cycling of marine DOC in the ocean. This work demonstrates that atomic force microscopy can facilitate structure determination in oceanic mixtures and provide an additional complimentary toolbox for analytical techniques in geophysical relevant environments.

1. Introduction

The marine dissolved organic carbon (DOC) reservoir is about 200 times larger than the living biosphere and similar in size to the atmospheric CO_2 pool (Hansell et al., 2009). Marine DOC is operationally defined as organic carbon passing through a 0.2–0.7 μm filter. The majority of DOC is presumed to originate from surface ocean primary production, because the stable isotopic signature of DOC is relatively homogeneous, and similar to that of marine phytoplankton (Williams, 1968). Thus, recently produced DOC has modern radiocarbon (^{14}C) ages similar to that of dissolved inorganic carbon (Beaupré & Aluwihare, 2010; Walker, Primeau, et al., 2016). Paradoxically, the mean ^{14}C age of deep DOC, ranging from 4000 to 6,400 ^{14}C years in the Atlantic to Pacific (Druffel & Griffin, 2015; Druffel et al., 2016), indicates that a portion of DOC survives multiple deep ocean mixing cycles. To explain this enigma, there are two DOC cycling paradigms. The dilution hypothesis proposes that all DOC molecules are intrinsically labile. However, the high molecular diversity and dilute concentration of these molecules create a "dilution threshold" that exerts a primary control on DOC cycling by limiting the probability of molecular interaction with microbes (Arrieta et al., 2015; Barber, 1968; Dittmar, 2015). Alternatively, a growing body of molecular-composition, incubation, and ^{14}C studies suggest that structural recalcitrance (i.e., the chemical composition and molecular structure of DOC molecules) predominantly controls the long-term persistence of DOC in the deep ocean (Benner & Amon, 2015; Jiao et al., 2010; Walker, Beaupre, et al., 2016).

While dilution and structural recalcitrance are not mutually exclusive (Jiao et al., 2014; Wilson & Arndt, 2017), studies that can further constrain DOC molecular structures will aid in understanding the relative role each mechanism plays in determining the long-term persistence of DOC.

To date, only a small fraction (~10%) of DOC can be readily identified as biomolecules, such as amino acids, sugars, lipids, and fatty acids (Kaiser & Benner, 2009). It is difficult to characterize DOC on a molecular level because DOC is a heterogeneous mixture in a highly saline solution. Ultrahigh-resolution mass spectrometry (Fourier-transform ion cyclotron resonance mass spectrometry, FT-ICR-MS; T. Dittmar & Stubbins, 2014; Koch & Dittmar, 2006) and multidimensional nuclear magnetic resonance spectroscopy have revealed thousands of structural features in DOC, and the presence of more than 5,000 molecular formulas (Hertkorn et al., 2006, 2013). However, the ability to unambiguously identify molecular structures by the formulas of the molecules is not straightforward, because the theoretically possible structural isomers per molecular formula exceed many millions (Hertkorn et al., 2006). The portion of DOC that is not ionized is also not known. From these techniques, high molecular weight (HMW) DOC was estimated to contain 8% carboxylic-rich alicyclic structures (CRAM), while the surface DOC contained polar biopolymers such as carbohydrates (Benner et al., 1992; Hertkorn et al., 2006).

Scanning probe microscopy is a powerful tool to directly image single molecules at the atomic scale. Recently, atomic force microscopy (AFM) with CO-functionalized tips demonstrated the real-space visualization of the chemical structure of molecules (Gross et al., 2009). The methodology has since been applied to different molecular systems, ranging from on-surface chemical reactions (de Oteyza et al., 2013; Kawai et al., 2016; Pawlak et al., 2017; Riss et al., 2016; Schuler et al., 2016; Schulz et al., 2017; van der Lit et al., 2013) to natural products (Gross et al., 2010; Hanssen et al., 2012; Hinaut et al., 2018; Schuler et al., 2015; Schuler, Fatayer, et al., 2017). A fraction of DOC has been previously characterized by AFM (Maurice & Namjesnik-Dejanovic, 1999; Pan et al., 2008). However, atomic resolution was not achieved.

Here, we report the first structurally discerned images of surface and deep DOC from the North Central Pacific Ocean using atomic-resolution low-temperature AFM. We analyzed unique low molecular weight (LMW) DOC samples extracted from both the surface and deep ocean (Broek et al., 2017) and determined the structures present in the background, refractory DOC pool, which likely represents the oldest marine ocean DOC (Beaupré & Aluwihare, 2010). LMW DOC consists of the refractory and ultra-refractory compounds (Benner & Amon, 2015; Walker et al., 2011) with old ^{14}C ages (Broek et al., 2017; Walker et al., 2011; Walker, Beaupre, et al., 2016) responsible for its long-term stability. Two previously characterized LMW DOC samples, collected from surface (7.5 m) and deep (2,500 m) waters of the North Pacific Ocean, were selected for this study. These samples were collected with a combined ultrafiltration and solid-phase extraction (SPE) approach (Broek et al., 2017), thus allowing for unambiguous isolation and characterization of LMW DOC. Chemical structure assignment of individual molecules was based on previous AFM image studies of model molecules with different planar aromatic hydrocarbon cores and diverse moieties (Gross et al., 2010; Kawai et al., 2016; van der Lit et al., 2013; de Oteyza et al., 2013; Riss et al., 2016; Schuler et al., 2015, 2016; Schuler, Fatayer, et al., 2017; Schuler, Zhang, et al., 2017).

2. Materials and Methods

2.1. Sample Collection

Seawater samples were collected aboard the *R/V* Kilo Moana in May 2015 during the research cruise KM1506. Sampling was conducted at the Hawaii Ocean Time Series station ALOHA (A Long-Term Oligotrophic Habitat Assessment; 22°45′N, 158°00′W). Surface water was collected via the vessel's underway sampling system through an intake pipe situated approximately 7.5 m below the waterline. Deep ocean (2,500 m) seawater was collected via successive casts of a rosette equipped with 12 × 24 L Niskin Bottles. LMW DOC was isolated as detailed in Broek et al. (2017). Briefly, seawater was filtered through a 0.2 μm cartridge filter and then ultrafiltered with 2.5 kD tangential flow ultrafiltration membranes in order to remove particles and HMW DOC, respectively. The permeate of the ultrafiltered system, containing only LMW DOC, was then acidified to pH 2 and concentrated by sorption onto a SPE resin (Agilent Bondesil PPL, 125 μm particle size, part #5982-0026). Ultrafiltration permeate (2,000–3,000 L) was loaded onto approximately 500 g of PPL SPE sorbent, equivalent to a loading of 2–3 mg-DOC per gram of sorbent. The sorbed LMW DOC was then desalted with ultrapure water and eluted from the SPE sorbent with methanol. These methanol-eluted solutions were

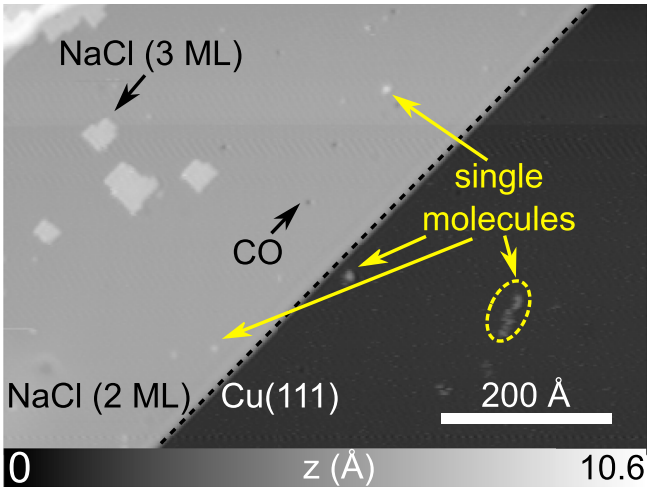

Figure 1. Scanning tunneling microscopy overview image of the sample preparation. Sample bias $V = 0.4$ V, tunneling current $I = 1$ pA.

then concentrated via rotary evaporation and subsequently dried to powder via centrifugal evaporation. Dry material was homogenized, transferred to precombusted (450 °C, 5 hr.) glass vials, and stored under desiccation until further analysis. A total of 15.5 μmol-DOC/l was recovered from the surface and 11.7 μmol-DOC/l from 2,500 m, representing (20 ± 1)% and (29 ± 5)% of total DOC respectively.

2.2. Scanning Probe Microscopy Experiments

The molecules to be studied were deposited on a Cu(111) single crystal, partially covered with bilayer NaCl as a substrate. The Cu(111) sample was cleaned by standard sputtering and annealing cycles. NaCl was evaporated at a sample temperature of 270 K to form bilayer islands (Bennewitz et al., 1999). Molecules were thermally evaporated from a silicon wafer by flash-heating onto the substrate (Schuler et al., 2015), kept at 10 K, to reduce surface diffusion of the molecules. That preparation led to a submonolayer coverage of separated molecules on the surface. Scanning probe microscopy experiments were performed using a home-built, combined scanning tunneling microscope (STM) and atomic force microscope based on a qPlus force sensor (Giessibl, 1998), operated in ultrahigh vacuum (10^{-10} mbar pressure) and at low temperature (5 K). The STM images were obtained in constant-current mode. All AFM images were obtained in the frequency-modulation mode (Albrecht et al., 1991; oscillation frequency of $f_0 = 30$ kHz and amplitude of $A = 0.5$ Å) in constant-height mode and at sample bias $V = 0$ V. The tip was functionalized with a CO molecule prior to molecular imaging (Bartels et al., 1997; Gross et al., 2009). Previously, AFM with CO-functionalized tips have been used to identify individual molecules of heavy oil fractions (Schuler et al., 2015; Schuler, Fatayer, et al., 2017). For these complex molecular mixtures, the comparison between the AFM-identified molecular structures and the distribution of carbon atom number and double-bond equivalent obtained by mass spectrometry demonstrated the representativeness of the AFM measurements (Schuler, Fatayer, et al., 2017). However, this representativeness is only given up to a maximum molecular weight lower than 1,000 g/mol, because of the preparation method used, which is by flash-heating a silicon wafer (Schuler et al., 2015). Molecules larger than 1,000 g/mol are usually fragmented in this preparation method before they sublime (Schuler et al., 2014). This restriction should represent no issue for the molecules studied here, with maximum molecular weights of about 300 g/mol observed. On the other hand, the samples investigated here contained many small molecules, which are mobile under the influence of the scanning probe tip even at $T = 5$ K and subpicoampere tunneling currents. These small, mobile molecules cannot be resolved by AFM or STM, and thus, the images shown are representative for the molecules in the samples that bonded strong enough to the NaCl and Cu surfaces to be imaged.

The AFM images show the frequency shift (Δf) as gray scale, where darker regions correspond to greater negative frequency shift. The images are obtained on the falling slope of $\Delta f(z)$ above the most protruding parts of the molecules (Gross et al., 2009). The tip height is typically chosen such that in the brightest regions (most repulsive interactions), the frequency shift is around $\Delta f = 0$ Hz or slightly positive by a few Hz. In the darkest regions Δf is typically on the order of -10 Hz.

The procedure for analyzing the molecular mixture on the surface consists of first surveying the surface with STM in a typical area of approximately 5,000 nm^2 as demonstrated in Figure 1. Afterward, each molecule in the surveying area is analyzed by constant-current STM and constant-height AFM.

3. Results

We resolved the molecular characteristics of the LMW North Pacific DOC (Broek et al., 2017) from the surface (S, 7.5 m) and deep (D, 2,500 m). To obtain a measure of the average sizes of the evaporated molecules, we measured 46 molecules in the surface sample S and 48 in the deep sample D by STM (Schuler, Fatayer, et al., 2017, and the supporting information). The average area size of the surveyed molecules S and D is quantified as (112 ± 60) $Å^2$ and (120 ± 60) $Å^2$, respectively. Therefore, within the area measurement limitation via STM, the average molecular area for both samples is equal. For both samples, most of the scanned molecules were mobile at the surface, being dragged by the STM tip while imaging. This could indicate nonplanar molecules

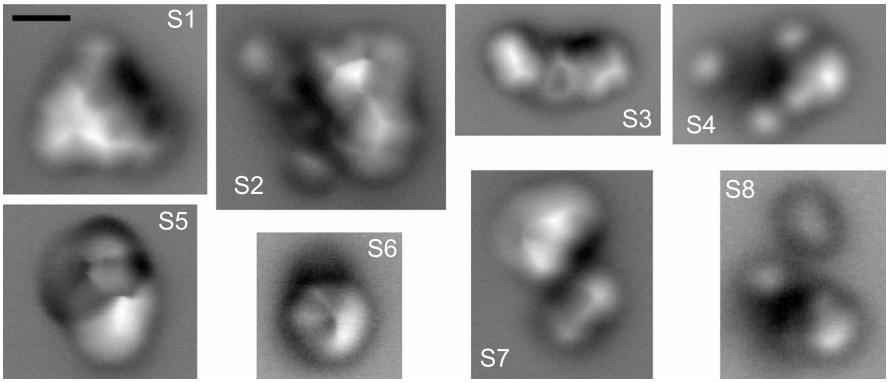

Figure 2. Atomic force microscopy images of the surface (S) North Pacific LMW DOC. Scale bar is 5 Å. All images have the same scale.

as well as molecules with larger side groups, such as alkane chains (Schuler, Zhang, et al., 2017). Moving molecules with the STM tip occurred even for mild experimental parameters such as tunneling currents of subpicoamperes. The molecules shown here are a representative random sample of the molecules that bonded to the Cu(111) and NaCl surfaces strongly enough to be imaged by AFM.

Constant-height AFM images from sample S are shown in Figure 2. Surface molecules were challenging to resolve with AFM, because most molecules possessed moieties that would protrude out of the surface and

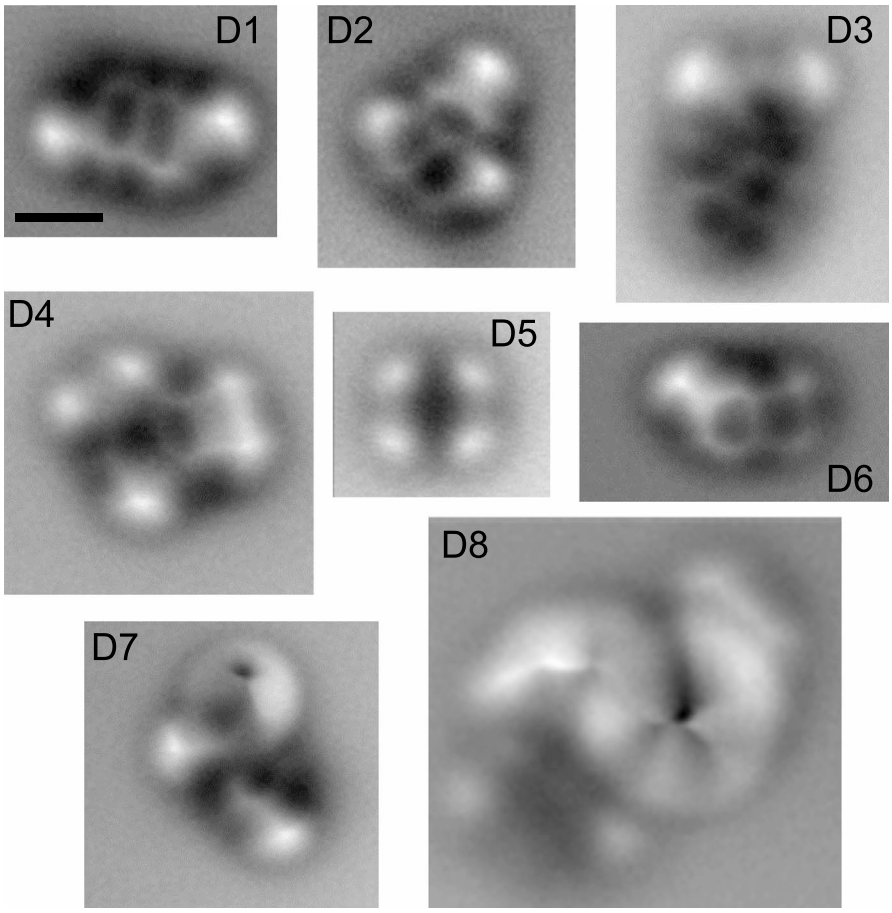

Figure 3. Atomic force microscopy images of deep (D) Pacific Ocean LMW DOC. Scale bar is 5 Å. All images have the same scale.

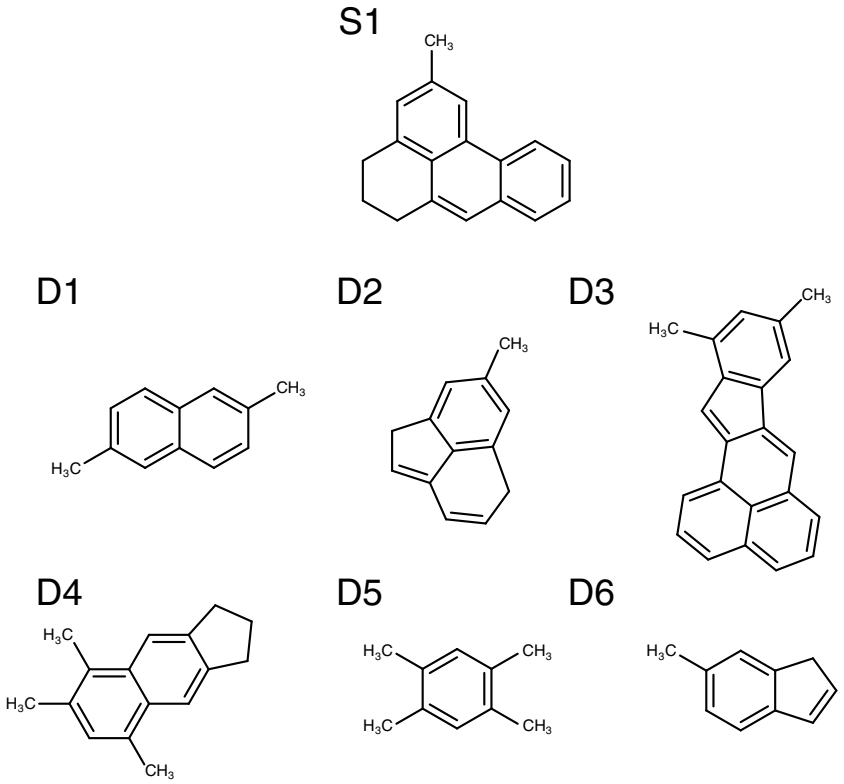

Figure 4. Assigned chemical structures for the surface (S1) and deep (D1–D6) Pacific LMW organic content. Molecules are identified as 5-methyl-5,6-dihydro-4H-benzo[a]phenalene (S1); 2,6-dimethylnaphthalene (D1); 7-methyl-1,5-dihydroacenaphthylene (D2); 1,3-dimethyl-indeno[2,1-a]phenalene (D3); 5,6,8-trimethyl-2,3-dihydro-1H-cyclopenta[b]naphthalene (D4); 1,2,4,5-tetramethylbenzene (D5); and 6-methyl-1H-indene (D6).

hinder the atomic resolution needed for the unambiguous interpretation of their chemical structures. In the surface, only ~8% of the measured molecules showed planar moieties that could be atomically resolved. Structures S1 through S3 were planar enough to be resolved well; at least one benzene ring from each of these structures was observed. The right side of the molecule S2 showcases a region where the repulsive interaction between tip and molecule, because of a protruding moiety, does not allow for unambiguous, complete structure elucidation. Molecules S5 to S8 exemplify molecules for which not even a partial chemical structure could be assigned by high-resolution AFM, also because of the presence of moieties protruding out of the surface.

Molecules from the deep were more suitable than those from the surface for characterization by high-resolution AFM (Figure 3). In the deep, approximately 20% of molecules were planar, and enabled structure elucidation by AFM imaging. Either a part of the planar aromatic core or the entire molecule was resolved by analyzing their frequency shift map. We observed single (D1) to quadruple (D5) methyl groups attached to the molecules as well as two (D1) to five (D3) carbon rings in the surveyed molecules. Molecules with functional groups that strongly interact with the CO-functionalized tip represent the majority of the measured molecules, such as molecules D7 and D8.

Additional insights for the chemical structure assignments can be gained by comparing the experimental AFM images with AFM simulations. The simulations use as input the hypothetical structure of a given molecule to calculate a map of the corresponding frequency shift by using the probe-particle model (Hapala et al., 2014; for the simulated AFM images see supporting information Figure S2). The assigned chemical structures are presented in Figure 4. Molecules are identified as 5,6-dihydro-4H-benzo[a]phenalene (S1); 2,6-dimethylnaphthalene (D1); 7-methyl-1,5-dihydroacenaphthylene (D2); 1,3-dimethyl-indeno[2,1-a]phenalene (D3); 5,6,8-trimethyl-2,3-dihydro-1H-cyclopenta[b]naphthalene (D4); 1,2,4,5-tetramethylbenzene (D5); and 6-methyl-1H-indene (D6).

Table 1
Structural Analysis of the Molecular Structures Inferred by High-Resolution AFM Imaging

Molecule	Molecular formula	Molecular formula (PAH core)	Molecular weight (g/mol)	Molecular weight (PAH core) (g/mol)	H/C	H/C (PAH core)	DBE	AI
D1	$C_{12}H_{12}$	$C_{10}H_8$	156.22	128.17	1.00	0.8	7	0.58
D2	$C_{13}H_{12}$	$C_{12}H_{10}$	168.23	154.21	0.92	0.84	8	0.62
D3	$C_{22}H_{16}$	$C_{20}H_{12}$	280.36	252.31	0.73	0.60	15	0.68
D4	$C_{16}H_{18}$	$C_{13}H_{12}$	210.31	168.23	1.13	0.92	8	0.50
D5	$C_{10}H_{14}$	C_6H_6	134.22	78.11	1.40	1	4	0.40
D6	$C_{10}H_{10}$	C_9H_8	130.19	116.16	1.00	0.89	6	0.60
S1	$C_{18}H_{16}$	$C_{17}H_{14}$	232.32	218.29	0.89	0.82	11	0.61

The structural information of the molecules identified by AFM imaging includes both samples and is presented in Table 1. The double bond equivalent varies between 4 (D5) to 15 (D3). The average double bond equivalent of the elucidated structures is 8.4 ± 3.6. The molecular weight varies from 130 Da (D6) to 280 Da (D3) and is on average 188 ± 56 Da. The H/C ratio of the polyaromatic hydrocarbon (PAH) core ranges from 1 (D5) to 0.6 (D3). The average H/C ratio of the PAH core is 0.84 ± 0.13. Considering the entire molecular structure, the H/C ratio ranges from 1.4 (D5) to 0.73 (D3). The average H/C ratio is 1.0 ± 0.2. The aromatic index (Koch & Dittmar, 2006) of our proposed structures ranges from 0.40 (D5) to 0.69 (D3). The average aromatic index is 0.6 ± 0.1.

We observed several differences between the samples collected at the surface and the deep. More three-dimensional structures were observed for the surface sample compared to the deep. On average, we find more PAHa, greater aromaticity, and less aliphatic moieties for the surveyed molecules from the deep. For this reason, only one molecule of the surface sample S could be assigned an unambiguous structure. However, the data for the many unassigned molecules in S enable us to draw the conclusion that those molecules feature nonplanar geometries with nonplanar carbon structures and an increased number of aliphatic moieties. This indicates a larger relative content of sp^3 hybridized carbon compared to the deep molecules (D). Second, the molecules we observe in the deep sample revealed several planar structures with aromatic sp^2 hybridized carbon frames, indicating an increased aromaticity of the molecules in the deep compared to those in the surface. We observe many five-membered carbon rings in the sample collected from the deep. We do not find any significant difference between the LMW size of surface and deep molecules given by STM area estimation (see supporting information Figure S1).

4. Discussion

We show that high-resolution AFM can be applied to study LMW DOC on an individual molecule basis. Although the molecular diversity of DOC is high, this single-molecule approach allows for the elucidation of chemical structures of selected individual planar DOC. We find molecules with less than five carbon rings, often containing a 5-membered ring within the assigned structures (Figures 2 and 3). In comparison with proposed structures on the basis of FT-ICR-MS experiments, our results support the presence of carboxylic-rich aliphatic structures CRAM (containing 5-membered rings) first identified by Hertkorn et al. (2006) in deep HMW DOC.

We also identified several planar PAH structures within the LMW DOC samples. The biochemical origin of such molecules is unclear, but the molecules share similar characteristics found in CRAM, and dissolved black carbon (BC). Dissolved BC is formed from the incomplete combustion of biomass and fossil fuels and is transported to the ocean by rivers, where a portion of BC cycles in DOC on millennial time scales (Coppola & Druffel, 2016; Jaffe et al., 2013; Ziolkowski & Druffel, 2010). Dissolved BC is the oldest identified compound in marine DOC and is refractory in the deep ocean (up to 23,000 ^{14}C years, 6 ± 2 % of DOC; Coppola & Druffel, 2016; Ziolkowski & Druffel, 2010).

Compared to other complex organic molecular mixtures found in nature, such as asphaltenes (Schuler et al., 2015) and heavy oil fractions (Schuler, Fatayer, et al., 2017), the molecules present in LMW DOC are smaller and less planar. Moreover, the DOC imaged also shows a higher incidence of methyl groups attached to the molecules and an increased occurrence of aliphatic groups in comparison to the asphaltenes. These

observations are consistent with many of the hypothesized complex aliphatic structures suggested by FT-ICR-MS work (Hertkorn et al., 2013). This is expected because of the different time scales involved in the respective chemical reactions and the much larger maturity of the asphaltenes (more than 10^6 years) compared to the marine DOC pool (10^3–10^5 years).

While our sample set is limited, the results here potentially have implications for understanding the relative importance of structural recalcitrance versus dilution as mechanisms for controlling the long-term persistence of deep ocean DOC. First, our LMW SPE DOC, by definition, has a high efficiency for extraction of LMW planar aromatic DOC. The surface and deep LMW DOC concentrations in this study are nearly identical ((15 ± 1) μmol/l for the surface, (12 ± 1) μmol/l for the deep; Broek et al., 2017). Thus, it is reasonable to assume that we can interpret the differences in % planar aromatic DOC between the two samples as a real compositional difference. As mentioned above, we find that surface LMW DOC has very few planar aromatics (~8%), and instead is composed of mostly 3-D structures. In contrast, deep LMW DOC has almost twice as many planar aromatic and CRAM-like molecules (20%). Deep LMW DOC $\Delta^{14}C$ values were also far more negative than surface LMW DOC (−578‰ and −343‰, respectively; Broek et al., 2017). These observations are consistent with both previous studies observing a buildup of CRAM and older DOC molecules at depth and largely support the hypothesis that structural recalcitrance controls the long-term persistence of DOC in the deep ocean (Benner et al., 1992; Flerus et al., 2012; Hertkorn et al., 2006; Jiao et al., 2010; Walker, Primeau, et al., 2016).

Although we have limited individual molecular diversity information from the two samples analyzed in this study, our results appear broadly inconsistent with dilution and molecular diversity as a principle control on LMW DOC cycling. The dilution hypothesis would predict deep LMW DOC to have a much higher molecular diversity of structures. However, of all 46 surface and 48 deep molecules, we imaged via AFM, none shared an identical structure. Thus, our results cannot confirm a change in overall molecular diversity with depth. If we consider planar aromatics as a "compound-class," the dilution hypothesis would predict the far more abundant planar aromatic DOC in the deep ocean to cycle more quickly since it is twice as concentrated as planar DOC in the surface ocean. It would also predict surface DOC (more diverse, 8% planar aromatics and mostly 3-D molecules) to cycle slower than deep DOC (less diverse, 20% planar aromatics). However, this interpretation is inconsistent with the negative LMW DOC $\Delta^{14}C$ values we observe at depth. Given these points, our results appear to be more consistent with structural recalcitrance as a predominant control on LMW DOC cycling.

5. Implications and Future Work

Our results provide the first real space images of single marine LMW DOC molecules with high-resolution AFM and offer insight into the biogeochemistry of marine aromatic compounds. Using North Pacific LMW DOC samples (Broek et al., 2017), we were able to directly evaluate selected planar structures of the more refractory LMW component of DOC. We show evidence that the majority of LMW DOC molecules feature a nonplanar geometry with nonplanar carbon structures and a significant content of aliphatic moieties. These observations are generally consistent with recent high-resolution FT-ICR-MS and nuclear magnetic resonance work suggesting a high diversity of aliphatic, and CRAM-like structures. At the same time, a surprising fraction of deep LMW DOC (~20%) could be identified as planar molecules (versus 8% in the surface). While the visualized structures are not representative of the entire sample, the difference in planar molecules observed could either reflect strong AFM interference by nonplanar molecules from the surface ocean or possibly suggest more dynamic cycling of LMW DOC molecules in the surface ocean, in contrast to the "refractory background" pool concept. Our deep LMW DOC results are consistent with the idea that structural recalcitrance exerts a primary control on deep DOC cycling. Future work can evaluate the recalcitrance of these structures directly using ^{14}C. Compound specific radiocarbon analysis of the individual aromatic rings in DOC can be extracted from DOC using a high temperature nitric acid digestion to liberate corresponding benzene polycarboxylic acids (Ziolkowski et al., 2011).

Future work based on high-resolution AFM can further increase the number of known chemical structures in LMW DOC. The expected increase in the understanding of the AFM contrast of different functional groups shall allow for more molecular structures to be discerned by AFM imaging in an ensemble of molecules, as the LMW DOC. Such knowledge would be based on imaging known standard molecules with different carbon ring connectivities (Schuler, Zhang, et al., 2017) as well as PAHs with different heteroatoms (Hapala

et al., 2016; Kocić et al., 2016). Another possible venue to be explored is the planarization of molecules via atom manipulation (Majzik et al., 2016). A planar specific stoichiometry pretreatment of DOC samples would allow for high recoveries of images of individual compounds. We suggest that this method can be applied to other ocean basins to investigate individual chemical structures present, which may be representatives of structural classes most responsible for the long-term stability of DOC in the refractory DOC pool.

Acknowledgments
The data contained in this article is available in the supporting information. The data can be visualized in an open software such as Gwyddion. We thank Rolf Allenspach for comments on the manuscript. The authors acknowledge financial support by the European Research Council (advanced grant "CEMAS"—agreement 291194 and consolidator grant "AMSEL"—agreement 682144) and EU projects "PAMS" (contract 610446) and initial training network "ACRITAS" (contract 317348). This work was also supported by University of Zurich Forschungskredit funding (A. I. C), National Science Foundation (NSF OCE-1358041, to M. C and T. B. and NSF OCE-1458941 to E. R. M. D.), and an American Chemical Society (ACS) Petroleum Research Fund (PRF) New Directions (ND) Grant (E. R. M. D. and B. D. W.). All authors contributed scientific comments and input on this manuscript. A. C., L. G., M. M., E. R. M. D., T. A. B., and B. D. W. contributed to the design of the study. S. F., F. S., G. M., and L. G. measured the samples and provided analytical assistance. S. F., A. C, L. G., M. M., B. D. W., T. A. B., and E. R. M. D. contributed to data interpretation. S. F., F. S., G. M., and L. G. designed the figures. Samples were provided by T. A. B. and M. M.

References

Albrecht, T. R., Grütter, P., Horne, D., & Rugar, D. (1991). Frequency modulation detection using high-Q cantilevers for enhanced force microscope sensitivity. *Journal of Applied Physics*, *69*(2), 668–673. https://doi.org/10.1063/1.347347

Arrieta, J. M., Mayol, E., Hansman, R. L., Herndl, G. J., Dittmar, T., & Duarte, C. M. (2015). Dilution limits dissolved organic carbon utilization in the deep ocean. *Science*, *348*(6232), 331–333. https://doi.org/10.1126/science.1258955

Barber, R. T. (1968). Dissolved organic carbon from deep waters resists microbial oxidation. *Nature*, *220*(5164), 274–275. https://doi.org/10.1038/220274a0

Bartels, L., Meyer, G., & Rieder, K.-H. (1997). Controlled vertical manipulation of single CO molecules with the scanning tunneling microscope: A route to chemical contrast. *Applied Physics Letters*, *71*(2), 213–215. https://doi.org/10.1063/1.119503

Beaupré, S. R., & Aluwihare, L. (2010). Constraining the 2-component model of marine dissolved organic radiocarbon. *Deep Sea Research Part II: Topical Studies in Oceanography*, *57*(16), 1494–1503. https://doi.org/10.1016/j.dsr2.2010.02.017

Benner, R., & Amon, R. M. W. (2015). The size-reactivity continuum of major bioelements in the ocean. *Annual Review of Marine Science*, *7*(1), 185–205. https://doi.org/10.1146/annurev-marine-010213-135126

Benner, R., Pakulski, J. D., Mccarthy, M., Hedges, J. I., & Hatcher, P. G. (1992). Bulk chemical characteristics of dissolved organic matter in the ocean. *Science*, *255*(5051), 1561–1564. https://doi.org/10.1126/science.255.5051.1561

Bennewitz, R., Barwich, V., Bammerlin, M., Loppacher, C., Guggisberg, M., Baratoff, A., et al. (1999). Ultrathin films of NaCl on Cu(111): A LEED and dynamic force microscopy study. *Surface Science*, *438*(1–3), 289–296. https://doi.org/10.1016/S0039-6028(99)00586-5

Broek, T. A. B., Walker, B. D., Guilderson, T. P., & McCarthy, M. D. (2017). Coupled ultrafiltration and solid phase extraction approach for the targeted study of semi-labile high molecular weight and refractory low molecular weight dissolved organic matter. *Marine Chemistry*, *194*, 146–157. https://doi.org/10.1016/j.marchem.2017.06.007

Coppola, A. I., & Druffel, E. R. M. (2016). Cycling of black carbon in the ocean: Cycling of black carbon in the ocean. *Geophysical Research Letters*, *43*, 4477–4482. https://doi.org/10.1002/2016GL068574

de Oteyza, D. G., Gorman, P., Chen, Y.-C., Wickenburg, S., Riss, A., Mowbray, D. J., et al. (2013). Direct imaging of covalent bond structure in single-molecule chemical reactions. *Science*, *340*(6139), 1434–1437. https://doi.org/10.1126/science.1238187

Dittmar, T. (2015). Reasons behind the long-term stability of dissolved organic matter. In *Biogeochemistry of Marine Dissolved Organic Matter* (pp. 369–388). Oxford, UK: Elsevier. Retrieved from http://linkinghub.elsevier.com/retrieve/pii/B9780124059405000078

Dittmar, T., & Stubbins, A. (2014). Dissolved organic matter in aquatic systems. In *Treatise on Geochemistry* (pp. 125–156). Oxford, UK: Elsevier. Retrieved from http://linkinghub.elsevier.com/retrieve/pii/B978008095975701010X

Druffel, E. R. M., & Griffin, S. (2015). Radiocarbon in dissolved organic carbon of the South Pacific Ocean. *Geophysical Research Letters*, *42*, 4096–4101. https://doi.org/10.1002/2015GL063764

Druffel, E. R. M., Griffin, S., Coppola, A. I., & Walker, B. D. (2016). Radiocarbon in dissolved organic carbon of the Atlantic Ocean. *Geophysical Research Letters*, *43*, 5279–5286. https://doi.org/10.1002/2016GL068746

Flerus, R., Lechtenfeld, O. J., Koch, B. P., McCallister, S. L., Schmitt-Kopplin, P., Benner, R., et al. (2012). A molecular perspective on the ageing of marine dissolved organic matter. *Biogeosciences*, *9*(6), 1935–1955. https://doi.org/10.5194/bg-9-1935-2012

Giessibl, F. J. (1998). High-speed force sensor for force microscopy and profilometry utilizing a quartz tuning fork. *Applied Physics Letters*, *73*(26), 3956–3958. https://doi.org/10.1063/1.122948

Gross, L., Mohn, F., Moll, N., Liljeroth, P., & Meyer, G. (2009). The chemical structure of a molecule resolved by atomic force microscopy. *Science*, *325*(5944), 1110–1114. https://doi.org/10.1126/science.1176210

Gross, L., Mohn, F., Moll, N., Meyer, G., Ebel, R., Abdel-Mageed, W. M., & Jaspars, M. (2010). Organic structure determination using atomic-resolution scanning probe microscopy. *Nature Chemistry*, *2*(10), 821–825. https://doi.org/10.1038/nchem.765

Hansell, D., Carlson, C., Repeta, D., & Schlitzer, R. (2009). Dissolved organic matter in the ocean: A controversy stimulates new insights. *Oceanography*, *22*(4), 202–211. https://doi.org/10.5670/oceanog.2009.109

Hanssen, K. Ø., Schuler, B., Williams, A. J., Demissie, T. B., Hansen, E., Andersen, J. H., et al. (2012). A combined atomic force microscopy and computational approach for the structural elucidation of Breitfussin A and B: Highly modified halogenated dipeptides from *Thuiaria breitfussi*. *Angewandte Chemie International Edition*, *51*(49), 12,238–12,241. https://doi.org/10.1002/anie.201203960

Hapala, P., Kichin, G., Wagner, C., Tautz, F. S., Temirov, R., & Jelínek, P. (2014). Mechanism of high-resolution STM/AFM imaging with functionalized tips. *Physical Review B*, *90*(8). https://doi.org/10.1103/PhysRevB.90.085421

Hapala, P., Švec, M., Stetsovych, O., van der Heijden, N. J., Ondráček, M., van der Lit, J., et al. (2016). Mapping the electrostatic force field of single molecules from high-resolution scanning probe images. *Nature Communications*, *7*, 11560. https://doi.org/10.1038/ncomms11560

Hertkorn, N., Benner, R., Frommberger, M., Schmitt-Kopplin, P., Witt, M., Kaiser, K., et al. (2006). Characterization of a major refractory component of marine dissolved organic matter. *Geochimica et Cosmochimica Acta*, *70*(12), 2990–3010. https://doi.org/10.1016/j.gca.2006.03.021

Hertkorn, N., Harir, M., Koch, B. P., Michalke, B., & Schmitt-Kopplin, P. (2013). High-field NMR spectroscopy and FTICR mass spectrometry: Powerful discovery tools for the molecular level characterization of marine dissolved organic matter. *Biogeosciences*, *10*(3), 1583–1624. https://doi.org/10.5194/bg-10-1583-2013

Hinaut, A., Meier, T., Pawlak, R., Feund, S., Jöhr, R., Kawai, S., et al. (2018). Electrospray deposition of structurally complex molecules revealed by atomic force microscopy. *Nanoscale*, *10*(3), 1337–1344. https://doi.org/10.1039/C7NR06261C

Jaffe, R., Ding, Y., Niggemann, J., Vahatalo, A. V., Stubbins, A., Spencer, R. G. M., et al. (2013). Global charcoal mobilization from soils via dissolution and riverine transport to the oceans. *Science*, *340*(6130), 345–347. https://doi.org/10.1126/science.1231476

Jiao, N., Herndl, G. J., Hansell, D. A., Benner, R., Kattner, G., Wilhelm, S. W., et al. (2010). Microbial production of recalcitrant dissolved organic matter: Long-term carbon storage in the global ocean. *Nature Reviews Microbiology*, *8*(8), 593–599. https://doi.org/10.1038/nrmicro2386

Jiao, N., Robinson, C., Azam, F., Thomas, H., Baltar, F., Dang, H., et al. (2014). Mechanisms of microbial carbon sequestration in the ocean – future research directions. *Biogeosciences*, *11*(19), 5285–5306. https://doi.org/10.5194/bg-11-5285-2014

Kaiser, K., & Benner, R. (2009). Biochemical composition and size distribution of organic matter at the Pacific and Atlantic time-series stations. *Marine Chemistry*, *113*(1–2), 63–77. https://doi.org/10.1016/j.marchem.2008.12.004

Kawai, S., Haapasilta, V., Lindner, B. D., Tahara, K., Spijker, P., Buitendijk, J. A., et al. (2016). Thermal control of sequential on-surface transformation of a hydrocarbon molecule on a copper surface. *Nature Communications*, *7*, 12711. https://doi.org/10.1038/ncomms12711

Koch, B. P., & Dittmar, T. (2006). From mass to structure: An aromaticity index for high-resolution mass data of natural organic matter. *Rapid Communications in Mass Spectrometry*, *20*(5), 926–932. https://doi.org/10.1002/rcm.2386

Kocić, N., Liu, X., Chen, S., Decurtins, S., Krejčí, O., Jelínek, P., et al. (2016). Control of reactivity and regioselectivity for on-surface dehydrogenative aryl–aryl bond formation. *Journal of the American Chemical Society*, *138*(17), 5585–5593. https://doi.org/10.1021/jacs.5b13461

Majzik, Z., Cuenca, A. B., Pavliček, N., Miralles, N., Meyer, G., Gross, L., & Fernández, E. (2016). Synthesis of a naphthodiazaborinine and its verification by planarization with atomic force microscopy. *ACS Nano*, *10*(5), 5340–5345. https://doi.org/10.1021/acsnano.6b01484

Maurice, P. A., & Namjesnik-Dejanovic, K. (1999). Aggregate structures of sorbed humic substances observed in aqueous solution. *Environmental Science & Technology*, *33*(9), 1538–1541. https://doi.org/10.1021/es981113

Pan, B., Ghosh, S., & Xing, B. (2008). Dissolved organic matter conformation and its interaction with pyrene as affected by water chemistry and concentration. *Environmental Science & Technology*, *42*(5), 1594–1599. https://doi.org/10.1021/es702431m

Pawlak, R., Vilhena, J. G., Hinaut, A., Meier, T., Glatzel, T., Baratoff, A., et al. (2017). Conformation and mechanical response of spray deposited single strand DNA on gold. Retrieved from https://doi.org/arXiv:1709.03099

Riss, A., Paz, A. P., Wickenburg, S., Tsai, H.-Z., De Oteyza, D. G., Bradley, A. J., et al. (2016). Imaging single-molecule reaction intermediates stabilized by surface dissipation and entropy. *Nature Chemistry*, *8*(7), 678–683. https://doi.org/10.1038/nchem.2506

Schuler, B., Collazos, S., Gross, L., Meyer, G., Pérez, D., Guitián, E., & Peña, D. (2014). From perylene to a 22-ring aromatic hydrocarbon in one-pot. *Angewandte Chemie*, *126*(34), 9150–9152. https://doi.org/10.1002/ange.201403707

Schuler, B., Fatayer, S., Meyer, G., Rogel, E., Moir, M., Zhang, Y., et al. (2017). Heavy oil based mixtures of different origins and treatments studied by atomic force microscopy. *Energy & Fuels*, *31*(7), 6856–6861. https://doi.org/10.1021/acs.energyfuels.7b00805

Schuler, B., Fatayer, S., Mohn, F., Moll, N., Pavliček, N., Meyer, G., et al. (2016). Reversible Bergman cyclization by atomic manipulation. *Nature Chemistry*, *8*(3), 220–224. https://doi.org/10.1038/nchem.2438

Schuler, B., Meyer, G., Peña, D., Mullins, O. C., & Gross, L. (2015). Unraveling the molecular structures of asphaltenes by atomic force microscopy. *Journal of the American Chemical Society*, *137*(31), 9870–9876. https://doi.org/10.1021/jacs.5b04056

Schuler, B., Zhang, Y., Collazos, S., Fatayer, S., Meyer, G., Pérez, D., et al. (2017). Characterizing aliphatic moieties in hydrocarbons with atomic force microscopy. *Chemical Science*, *8*(3), 2315–2320. https://doi.org/10.1039/C6SC04698C

Schulz, F., Jacobse, P. H., Canova, F. F., van der Lit, J., Gao, D. Z., van den Hoogenband, A., et al. (2017). Precursor geometry determines the growth mechanism in graphene nanoribbons. *The Journal of Physical Chemistry C*, *121*(5), 2896–2904. https://doi.org/10.1021/acs.jpcc.6b12428

van der Lit, J., Boneschanscher, M. P., Vanmaekelbergh, D., Ijäs, M., Uppstu, A., Ervasti, M., et al. (2013). Suppression of electron–vibron coupling in graphene nanoribbons contacted via a single atom. *Nature Communications*, *4*. https://doi.org/10.1038/ncomms3023

Walker, B. D., Beaupré, S. R., Guilderson, T. P., Druffel, E. R. M., & McCarthy, M. D. (2011). Large-volume ultrafiltration for the study of radiocarbon signatures and size vs. age relationships in marine dissolved organic matter. *Geochimica et Cosmochimica Acta*, *75*(18), 5187–5202. https://doi.org/10.1016/j.gca.2011.06.015

Walker, B. D., Beaupré, S. R., Guilderson, T. P., McCarthy, M. D., & Druffel, E. R. M. (2016). Pacific carbon cycling constrained by organic matter size, age and composition relationships. *Nature Geoscience*, *9*(12), 888–891. https://doi.org/10.1038/ngeo2830

Walker, B. D., Primeau, F. W., Beaupré, S. R., Guilderson, T. P., Druffel, E. R. M., & McCarthy, M. D. (2016). Linked changes in marine dissolved organic carbon molecular size and radiocarbon age. *Geophysical Research Letters*, *43*, 10,385–10,393. https://doi.org/10.1002/2016GL070359

Williams, P. M. (1968). Stable carbon isotopes in the dissolved organic matter of the sea. *Nature*, *219*(5150), 152–153. https://doi.org/10.1038/219152a0

Wilson, J. D., & Arndt, S. (2017). Modeling radiocarbon constraints on the dilution of dissolved organic carbon in the deep ocean. *Global Biogeochemical Cycles*, *31*, 775–786. https://doi.org/10.1002/2016GB005520

Ziolkowski, L. A., Chamberlin, A. R., Greaves, J., & Druffel, E. R. M. (2011). Quantification of black carbon in marine systems using the benzene polycarboxylic acid method: A mechanistic and yield study. *Limnology and Oceanography-Methods*, *9*, 140–149. https://doi.org/10:4319/lom.2011.9.140

Ziolkowski, L. A., & Druffel, E. R. M. (2010). Aged black carbon identified in marine dissolved organic carbon. *Geophysical Research Letters*, *37*, L16601. https://doi.org/10.1029/2010GL043963